RESEARCH PAPER

Influence of load-level and effective thickness on the fire resistance of composite slabs with steel deck

Lucas Santos[1], Paulo A. G. Piloto[2,], Carlos Balsa[2], Érica F. A. Kimura[1]*

[1]Universidade Tecnológica Federal do Paraná, Curitiba, Brazil
[2]Instituto Politécnico de Bragança, Bragança, Portugal

Abstract

Composite slabs with steel deck have been used on building construction due to its fast-and-easy crafting that brings economic outstanding alternatives to architects and engineers on large-scale steel framed constructions. At room temperatures and in Europe, the designing procedures of composite slabs are defined by Eurocode 1994-1-1. When it comes to the fire safety analysis of these elements, the designing procedure requires more attention due to the direct exposition of the steel deck to fire, affecting the overall bending resistance. This importance is presented in Eurocode 1994-1-2, taking in consideration the integrity, insulation and load-bearing criteria. In this work the thermal and mechanical behavior of composite slabs with steel deck exposed to standard fire ISO 834 are studied through numerical simulations using Finite-Element Method (FEM). The model was previously validated with one experimental test from literature. The ANSYS Mechanical APDL software was used to develop a parametric study, simulating four different geometries with different load levels, comprehending a total of 126 thermal and mechanical simulations used to determine the correlation between load-level and fire resistance. As result, a new simplified method is proposed for the load bearing fire resistance of composite slabs, considering the effect of the effective thickness and the load level. The fire resistance decreases with the load level and increases with the thickness of the concrete. A new proposal is presented to determine the fire resistance, based on these two parameters.
Keywords: Composite slabs, Steel deck, Load level, Fire resistance, Numerical simulations

Introduction

The building industry shows constant development and presents new technologies that contributes to foster this construction sector. As required by fire engineering principles, the constructions elements must provide the required level of safety. Since last decades, large and tall building construction sector have been replacing the conventional concrete slabs by composite slabs with steel deck. This solution brings faster, easier and cheaper slabs to large scale buildings, given that the same steel deck is used as concrete formworks, working as a composite layer element, as shown at Figure 1. The use of steel deck, as main positive bending reinforcement component, allows the reduction of the amount of rebars usually applied within traditional concrete slabs, but turns this reinforcement directly exposed to fire from bellow.

Aiming to guide the safety design and use of this technology, in 1983 the European Convention for Constructional Steelwork (ECCS) published the first technical note for the calculation of fire resistance of composite concrete slabs with profiled steel sheet [1], providing geometry requirements as the slab minimum height, for example, based on the desired fire resistance class to the element.

The classification of fire resistance of composite slabs might be done under experimental tests, exposing the structure to a standard fire from below and evaluating it under Integrity (E), Insulation (I) and Loadbearing (R) fire resistance criteria.

---

* Corresponding author. Tel.: +351-273303157; e-mail: ppiloto@ipb.pt

One of the first experimental tests were developed by Thomson et al. [2] and Cooke et al. [3], exploring the thermal and mechanical response of composite slabs with trapezoidal and re-entrant geometries, recording complete descriptions of the experiments and noticing that such standards showed up to be conservative.

During early 90's the research on this topic increased, with increasing number of experimental tests and the development of numerical models. In 1990, Hamerlinck and Stark [4] developed experiments tests which were used on the validation of the finite-element models. These models were able to predict with, good accuracy, the temperature and maximum deflection of the slabs during the tests. Both [5] in 1996, also developed experimental tests and numerical simulations, but additionally proposed simplified calculation models to determine the fire resistance of composite slabs. This simplified calculation model was then assumed in the European standard EN 1994-1-2 [6] and has been used to estimate the fire resistance of composite slabs, when using the insulation criterion.

Since then, researchers tried to evaluate the accuracy and improve the current version of EN 1994-1-2. Also, different numerical models were developed, providing better agreement with experimental test results, as demonstrated by Lim et al. [7] and Jiang et al. [8]. In 2019, Piloto et al. [9] developed several 2D numerical simulations and experimental tests, aiming to evaluate the fire performance of composite slabs under fire and validate the numerical model with air gap effect. In 2020, Piloto et al. [10] developed 3D FEM models to simulate the existence of an air gap between the steel deck and the concrete topping, concluding that the airgap effect is fundamental to validate the numerical results. Based on the latter, a new formula was proposed for the calculation of the fire resistance, depending on the effective thickness of the composite slab and on the air gap thickness. Also, in 2020 Piloto et al. [11] developed the thermo-mechanical 3D numerical model capable of simulating the response of a composite slab with steel deck under fire, also validating this model with the experimental test developed by Hamerlinck [4, 12, 13].

This investigation is in line with these previous studies and intends to verify the influence of the load level in the fire resistance, when evaluated under the insulation and the loadbearing criteria. Authors use the same software to develop a parametric analysis, using different steel deck geometries and loading levels. Additional reference can be found regarding the numerical validation [14].

Fire Resistance: Eurocode 4

The design of composite slabs with steel deck at room temperature and under fire resistance conditions is defined by EN1994, parts 1.1 [15] and 1.2 [6], respectively. EN1994 part 1.2 provides the rules to design such composite elements within the fire safety criteria established by the general requirements for fire resistance tests [16], considering three fire rating domains: load bearing (R), integrity (E) and insulation (I). These fire ratings should agree with the fire classification of construction products and building elements [17].

The integrity criterion (E) measures the capacity of the structure on preventing the passage of hot gases or flames from the exposed to the unexposed surface of the slab [16] and it is normally satisfied as long as (I) an (R) criteria are sustained, given that the steel deck acts as a membrane-like to the composite slab. The current version of the standard used for determining the fire resistance of composite slabs under standard fire [16] has been changing quite often, in particular with respect to flexural loaded elements (R). For the insulation criterion (I) the standard has been kept for long time.
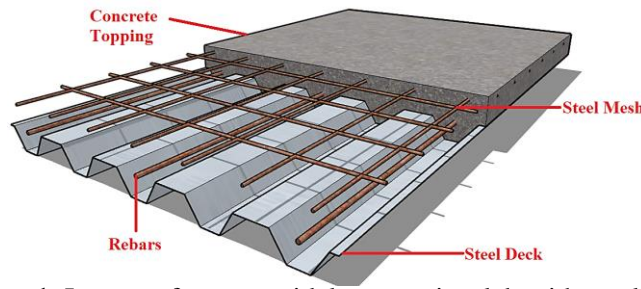
**Figure 1.** Layout of a trapezoidal composite slab with steel deck.

Insulation (I)

According to the European standard used for fire resistance tests [16], the insulation (I) criterion is the slab's ability of limit the temperature rise on the unexposed surface, below 180°C to the maximum temperature or, below 140°C to the average temperature, relative to the initial average temperature. The EN1994 part 1.2 [6], Annex D, specifies a simplified method to estimate the fire resistance (t_i) of unprotected composite slabs, considering the insulation criterion. The Equation (1) must be used, taking in consideration the geometric characteristics of the slab as shown in Figure2.

$$t_i = a_0 + a_1.h_1 + a_2.\phi_{upper} + a_3 \frac{A}{L_r} + a_4 \frac{1}{l_3} + a_5 \frac{A}{L_r} \frac{1}{l_3} \tag{1}$$

The geometry factor of the rib A/Lr shall be calculated using Equation (2).

$$\frac{A}{L_r} = \frac{h_2 \cdot \left(\frac{l_1 + l_2}{2}\right)}{l_2 + 2\sqrt{h_2^2 + \left(\frac{l_1 - l_2}{2}\right)^2}} \tag{2}$$
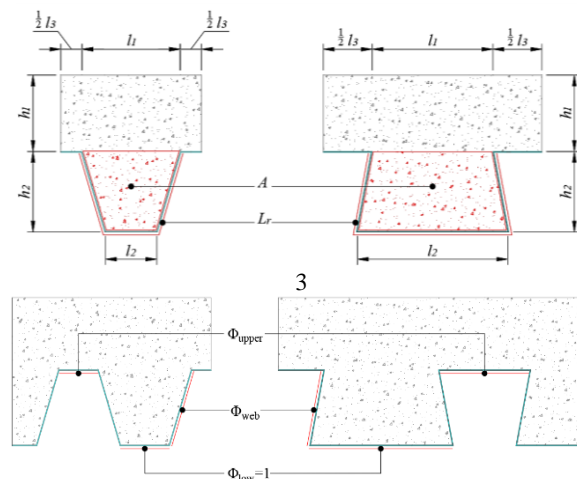
Figure 2. (a) Geometry of the composite slabs; (b) View factors used for radiation.

Furthermore, ϕ_{upper} is the view factor of the upper flange of the steel deck and the empirical coefficients a_i are concrete-density-type dependent, as shown on Table 1 (NWC – Normal Weight Concrete, LWC- Low Weight Concrete). The view factor ϕ quantifies the geometric relation between the surface emitting radiation and the surface receiving. It depends on the distance between surfaces, as well as area and orientation.

Table 1. Coefficients for estimating the fire resistance ti (EN 1994-1-2 [6]).

Concrete Type	a_0(min)	a_1(min/mm)	a_2(min)	a_3(min/mm)	a_4(mm*min)	a_5(min)
NWC	-28.8	1.55	-12.60	0.33	-735	48.0
LWC	-79.2	2.18	-2.44	0.56	-542	52.3

Three different average view factors may be considered for numerical simulation, assuming three steel deck components: the upper flange view factor (ϕ_{upper}) and the web view factor (ϕ_{web}), which can be estimated by Equation (3) and Equation (4), following the Hottel's crossed-string method, respectively. The lower flange view factor (ϕ_{low}), is usually considered equal to 1, when considering it is directly exposure to fire.

$$\phi_{upper} = \frac{\sqrt{h_2^2 + \left(l_3 + \frac{l_1 - l_2}{2}\right)^2} - \sqrt{h_2^2 + \left(\frac{l_1 - l_2}{2}\right)^2}}{l_3} \tag{3}$$

$$\phi_{web} = \frac{\sqrt{h_2^2 + \left(\frac{l_1 - l_2}{2}\right)^2} + (l_3 + l_1 - l_2) - \sqrt{h_2^2 + \left(l_3 + \frac{l_1 - l_2}{2}\right)^2}}{2\sqrt{h_2^2 + \left(\frac{l_1 - l_2}{2}\right)^2}} \tag{4}$$

To find the fire resistance (t_i) by numerical simulation, one needs to solve the second order differential equation for energy. The finite element method can be used with the corresponding boundary conditions, defined in EN1991-1.2 [18].

Load bearing (R)

The loadbearing criterion (R) measures the ability of the slab to support the load. This ability is determined from the measurements of the maximum deflection (D) and rate of deflection (dD/dt), following the definitions presented on Table 2, where L represents the clear span (mm) and d represents the distance in the cross section, from the extreme fibre of the cold design compression zone to the extreme fibre of the cold design tension zone.

Table 2. Definitions to find the load bearing capacity of bending elements.

Definition for limits	Expression	Unity
D_{lim}	$\dfrac{L^2}{400d}$	mm
$(dD/dt)_{lim}$	$\dfrac{L^2}{9000d}$	mm/min

Failure to support the test load has deemed to have occurred when one of the fowling conditions are verified:

$$D_{measure} \geq 1.5\, D_{lim} \tag{5}$$

$$D_{measure} \geq D_{lim} \quad \wedge \quad dD_{measure}/dt \geq (dD/dt)_{lim} \tag{6}$$

The EN1994 part 1.2, annex D, includes the prediction of the fire resistance with respect to the load bearing criterion, based on the calculation of the sagging and hogging moment. This method is based on the temperature prediction of all the four components of the composite slab (lower flange, web, upper flange and rebar), considering different fire ratings.

Assuming the simply supported condition for the composite slab, the sagging moment should be determined, according to Equation (7).

$$M_{fi,t,Rd} = \sum_{i=1}^{n=4} A_i \; z_i \; k_{y,\theta,i} \left(\frac{f_{y,i}}{\gamma_{M,fi}}\right) + \alpha_{slab} \sum_{j=1}^{m=1} A_j \; z_j \; k_{c,\theta,j} \left(\frac{f_{c,j}}{\gamma_{M,fi,c}}\right) \tag{7}$$

Based on each temperature component, the reduction coefficients ($k_{y,\theta,i}$) for the yielding stress ($f_{y,i}$) are determined, according to the behaviour of the steel components at elevated temperatures [19]. Also, in this calculation model, the concrete section in compression must be considered at ambient temperature, so strength-reduction coefficient $k_{c,\theta,j}$ is equal to unity. So, to each fire rating, the plastic neutral axis is required to find the design moment resistance, according to Equation 7, considering both loads: dead-load and living load.

Finite Element Model

The numerical models were developed with ANSYS Mechanical APDL, see Figure 3, keeping uniform modelling procedures such as, mesh size, material properties and boundary conditions. On this section these procedures are presented, including the numerical validation.

The dimension of the slab is 3.20 m long by 0.65 m wide. The slab is submitted to 4 lines of loading zones.
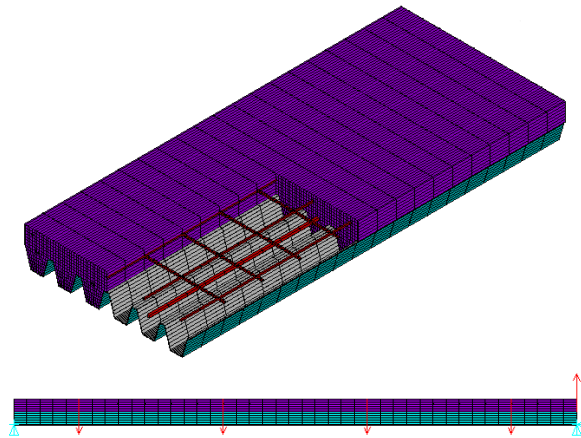
Figure 3. Finite element mesh of Hamerlinck's Test 2 experiment.

Thermal model

The thermal analysis comprises the simulation of the composite slab with standard fire from below. The full 3D modelling of the composite slab with steel deck is depicted on Figure 3. The simulation process requires the solution of a nonlinear transient thermal analysis, using 3D finite elements (SHELL 131, SOLID 70 and LINK 33). This solution process is incremental and iterative. The normal time step is 60 s, but can be reduced to 1 s. The convergence was achieved with heat flow, using a tolerance value of 0.001. The finite element method (FEM) requires the solution of Equation (8) in the domain and the definition of the boundary conditions according to Equation (9) in the exposed and unexposed side of the slab.

$$\nabla\left(\lambda_{(T)}.\nabla T\right) = \rho_{(T)}.Cp_{(T)}.\frac{\partial T}{\partial t} \tag{8}$$

$$\lambda_{(T)}.\nabla T.\vec{n} = \alpha_c\left(T_g - T\right) + \phi.\varepsilon_m.\varepsilon_f.\sigma.\left(T_g^4 - T^4\right) \tag{9}$$

whereas $\rho_{(T)}$ is the specific mass of each material, T is the temperature of each material, $C_{p(T)}$ is the specific heat, $\lambda_{(T)}$ is the thermal conductivity, α_c is the convection coefficient, T_g represents the gas temperature of the fire compartment, ε_m is the emissivity of each material, ε_f represents the emissivity of the fire, σ represents the Stefan-Boltzmann constant (5.67x10-8 $W/m^2\ K^4$) and ϕ is the view factor of the component.

The finite element SOLID70 was selected to model the concrete, which consists in a solid hexahedron with 8-nodes, with a single degree of freedom (DOF) at each node. Linear interpolating functions are used for this element and the full Gauss integration method is applied (2x2x2). Rebars and steel mesh reinforcement were represented by linear LINK33 elements, using two nodes and one DOF per node. This element uses exact integration method.

The finite element SHELL131 was selected to model the steel deck and the air gap. This element is made by 4 nodes, with up to 32 DOF at each node, depending on the number of layers used. This element uses linear interpolation between nodal temperatures and full integration (2x2) in the plane of the shell and 3 integration points through the thickness.

For the parametric analysis, perfect contact is assumed between all the materials, using one single layer for the element SHELL131 to represent the steel deck. On the other hand, for the validation process, an alternative model is proposed, using an extra layer for the element SHELL131 to simulate the air gap. This air gap is a result of the detachment of the steel deck from the concrete topping, usually verified and reported by other researchers, such as [12, 20, 21]. Both the validation model and parametric models were exposed to standard fire ISO 834 [22], following the recommendations of convection coefficients on the exposed surface (α_c=25 W/m²K) and unexposed surface (α_c=9 W/m²K) [18]. General boundary conditions are presented on Figure 4. Only convection is assumed in the unexposed surface, when assuming it contains the effects of heat transfer by radiation.
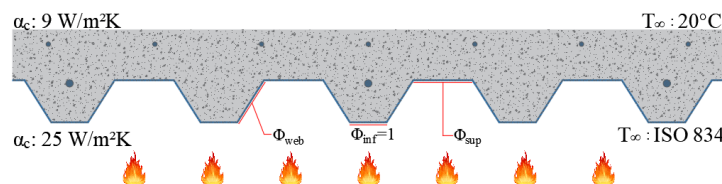
**Figure 4.** Boundary conditions on thermal simulations.

Mechanical model

The mechanical simulation requires changing element types, switching from thermal model to mechanical model. Boundary conditions should also be updated. Therefore, the concrete is simulated using SOLID185 and steel rebars and steel deck, are simulated with LINK180 and SHELL181, respectively. All these elements present linear interpolation functions with full integration schemes, except for LINK180 which includes exact integration. The supports were applied directly on nodes, as well as forces, as depicted in Figure 3. The gravity force (9.81 m/s²) was considered to model the dead load, affecting all the materials in the entire model.

Numerical validation

To evaluate the accuracy of the finite element model, the numerical validation is based on Hamerlinck's experimental test 2 [12].The experiment considers a simply supported composite slab (3.20 m long by 0.65 m wide), using PRINS PSV73 steel deck model with steel reinforcement provided by 10 mm rebars at the lower section and 6//150 mm steel mesh placed

20 mm beneath the top of the slab, as depicted on Figure 5. Also, normal weight concrete (NWC) from C20/25 class is used, with 3.4% moisture content.
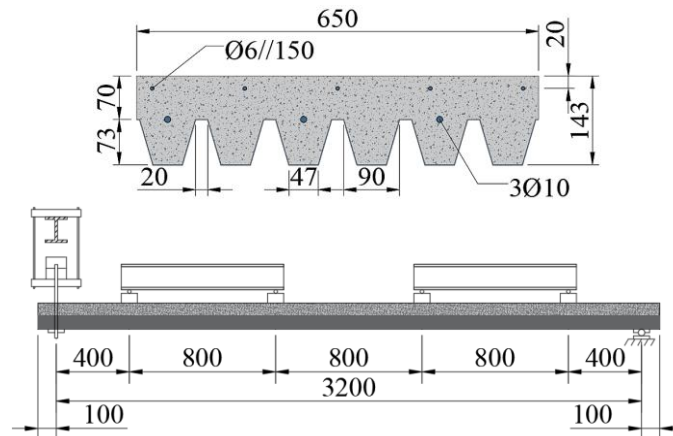

Figure 5. Geometry and loads used to validate Hamerlinck's Test 2 experiment.

The finite element model is presented in Figure 3. An extra layer has been used for the air gap effect, according to authors observation during the experimental test [12]. This extra layer was used during the thermal analysis, with SHELL131, and removed during the mechanical analysis. This additional layer introduces an average thermal resistance during the simulation of the experimental test. Two different air gap thickness have been tested (0.5 mm and 1.0 mm). The air gap model includes the simulation of heat flow by conduction, using the thermal properties at 1 atm pressure, presented by Çengel and Ghajar [23]. The validation is presented for the first analysis (thermal) and for the second analysis (mechanical). Figure 6 (a) presents the temperature evolution in single reference nodes of the numerical model in comparison to the experimental results, using the 0.5 mm airgap between steel sheet and concrete. Figure 6 (b) presents the comparison of vertical displacements and the rates of vertical displacement between the same model and the results provided by Hamerlinck [12].

The results are also presented for the fire resistance, determined by insulation (I) and load bearing (R): The results are presented for insulation in Table 3 and for load bearing in Table 4.

The air gap models show good approximation for the thermo-mechanical analysis, proving the ability of the proposed finite element modelling technique to simulate the debonding effect of the steel deck under fire.
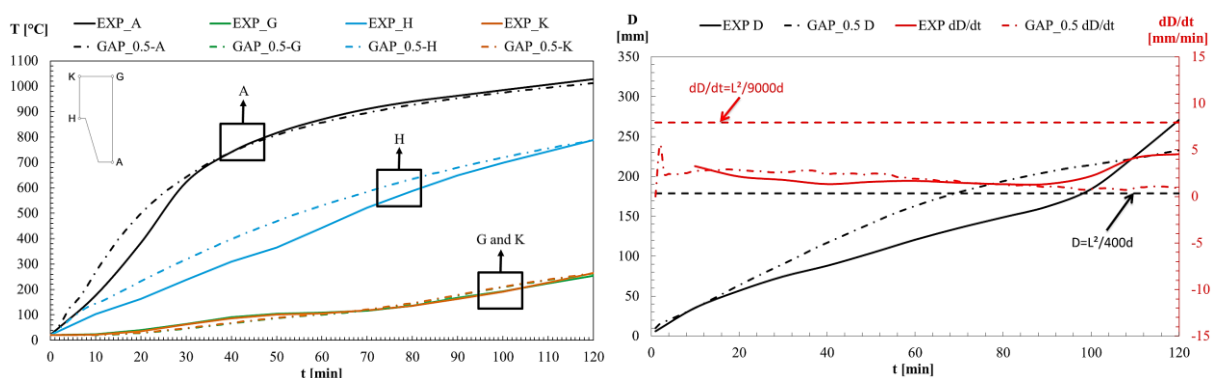
Figure 6. a) Temperatures, b) Displacement and rate of displacement at mid span of the slab.

Table 3. Fire resistance for insulation (t_i) of Test 2 composite slab.

Insulation Criteria	Numerical models – thermal analysis			Hamerlinck Experimental results
	PCM (Perfect Contact Model)	AIR-GAP_0.5 (0.5mm air-gap model)	AIR-GAP_1.0 (1.0mm air-gap model)	
$t_{i,ave}$	75.30	84.90	93.10	88.30
$t_{i,max}$	85.30	96.40	105.92	102.00
t_i deviation	-14.72%	-3.85%	+5.44%	-

Table 4. Fire resistance for load bearing (t_i) of Test 2 composite slab.

Insulation Criteria	Numerical models – thermo-mechanical analysis			Hamerlinck Experimental results
	PCM (Perfect Contact Model)	AIR-GAP_0.5 (0.5mm air-gap model)	AIR-GAP_1.0 (1.0mm air-gap model)	
$t_{r,D}$	54.50	69.10	81.10	97.60
$t_{r,D/dt}$	Not achieved	Not achieved	Not achieved	Not achieved
t_r deviation	-44.16%	-20.20%	-16.91%	-

Parametric study

A parametric study is presented to capture the effect of the load level and effective thickness on the fire resistance of composite slab with steel deck. The validation of the numerical model was essential and used as base to develop different models of slabs, that differ from each other on steel deck profile model, concrete topping height (h_1) and loading level (η), adding up to 120 simulations. The debonding effect was not included, because this effect depends on the characteristic of the application.

Models

The parametric analysis uses a composite slab with steel deck with 1 m wide and 3 m long, simply-supported, exposed to a standard fire ISO 834 [22] from below. Four different models of steel deck are presented, 2 trapezoidal (T1 and T2) and 2 re-entrant (R1 and R2), see Table 5. On each slab, three S500-class rebars, Ø10 mm, are equally spaced through the slab cross section at the height h_2 of each model and the additional S500-class steel mesh Ø6//150 mm is placed 20 mm under the top surface of concrete. The NWC concrete from C20/25 class is considered to fulfil the composite slabs with 3.00% moisture content. The steel grade for the deck changes in accordance to each steel deck type.

Table 5. Steel deck models used on the parametric study.

ID	Model	ϕ_{upper}	ϕ_{web}	Thickness (mm)	Concrete Class	Steel Grade Deck	Steel Grade Rebars
T1	Polideck 59S (Brazil)	0.78	0.67	1.25	NWC C20/25	S275	S500
T2	Cofraplus 60 (Poland)	0.73	0.56	1.25	NWC C20/25	S350	S500
R1	Multideck 50 (United Kingdom)	0.14	0.09	1.00	NWC C20/25	S450	S500
R2	Bondeck (Australia)	0.28	0.18	1.00	NWC C20/25	S350	S500

All the models were developed following the basic model proposed on Figure 7. Six different thicknesses (h_1=40…90mm) are considered and five different load levels (η_i= 40…80%) are used to study the effect of both parameters. The magnitude of the load applied is based on the load bearing capacity, previously determined at room temperature. The load (q) was distributed over the unexposed surface area, using nodal forces to guarantee a better load distribution during simulations.
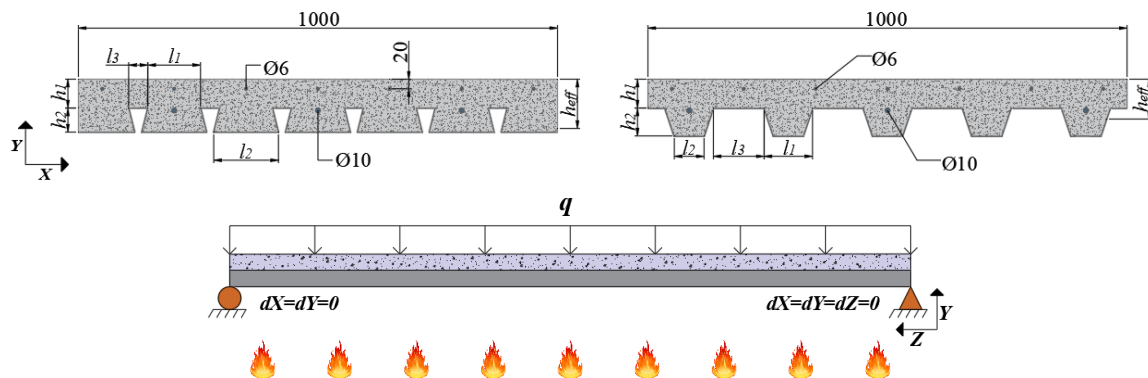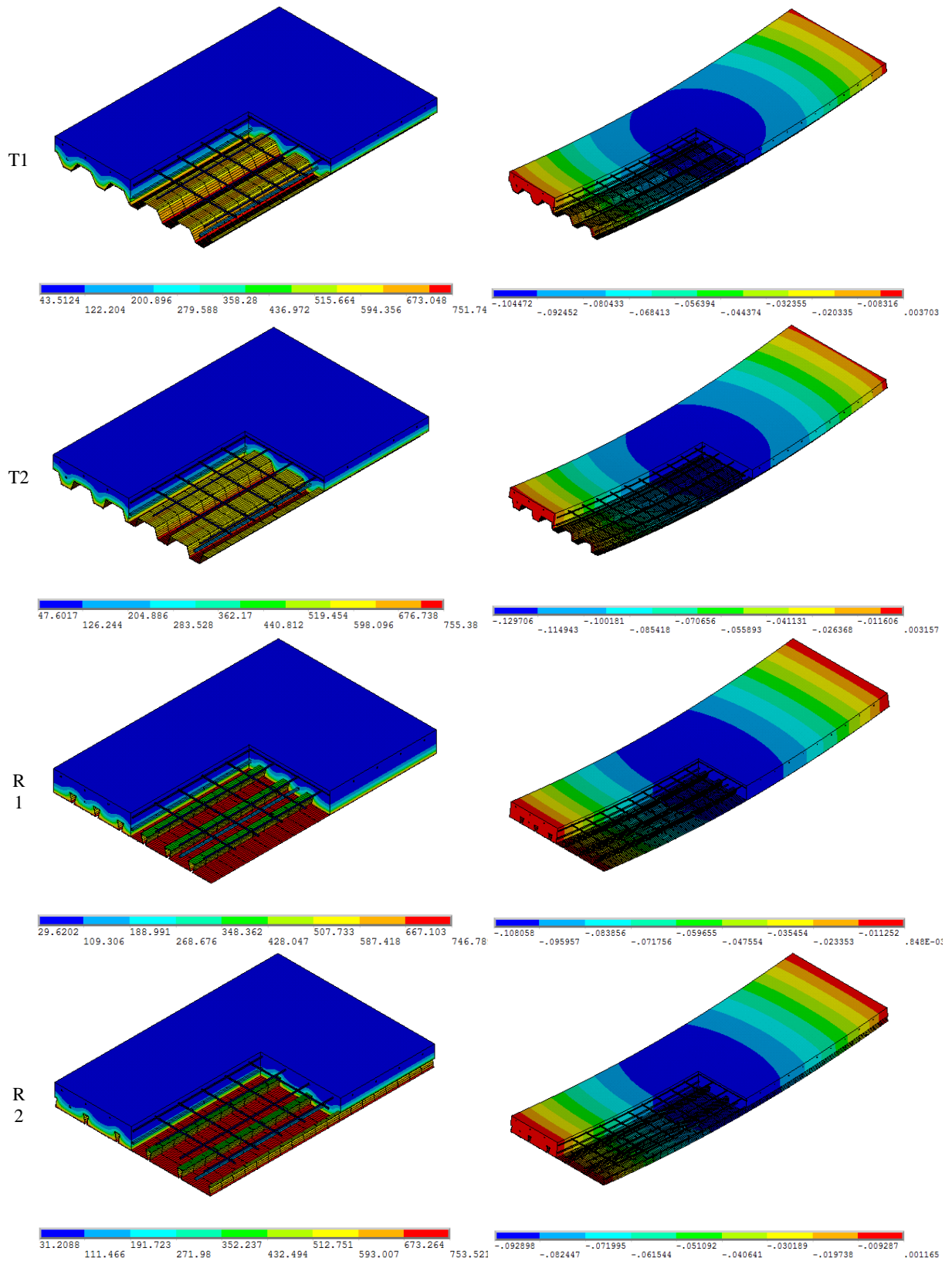

Figure 7. Trapezoidal and re-entrant models of composite slabs used on the parametric study.

Figure 8 presents one example of the main results determined from the thermal and thermo-mechanical analysis. The results are presented for a load level of 40% and for a concrete thickness h_1=80 mm, after 30 minutes of fire exposure.

The composite slab T2 presents the biggest displacement at mid span, while the composite slab R2 presents the smallest transversal displacement. Both re-entrant composite slabs, R1 and R2, present the lowest temperature in the unexposed side, which can be justified by the smallest view factors for the upper flange and web of the steel deck if compared to the trapezoidal, T1 and T2, models. Therefore, it appears that the re-entrant slabs are providing better thermal and mechanical performance after 30 minutes of fire exposure.

Figure 8. Temperature and displacement results after 30 minutes of fire exposure for both types of trapezoidal and re-entrant models.

Results

Based on the outputs of temperatures during the thermal simulations and deflections, at mid-span of the slabs, during the thermo-mechanical simulations, a compilation of fire resistance analysis (R) is presented, consider all the composite slabs. A new proposal is presented for the calculation of the fire resistance, taking int consideration the effective thickness and the load level.

Figure 9 shows the approximation surfaces generated by minimizing the difference between the numerical results and the new proposal. The new proposed equations, Equation (10) to Equation (13), are presented in Table 6. They were developed using the open source software GNU Octave, with 30 scatter points each, based on quadratic approximations to the effective thickness (h_{eff}) and the load level (η).

The surface approximation is adjusted to keep the safety level for this element, when estimating its fire resistance, guaranteeing that the real fire resistance of the composite slab should be equal or greater than the calculated. The margin of error is 4 minutes to composite slabs with T1, 13 minutes to slabs using T2 steel sheet profile, 11 minutes to the structures composed with T2 steel deck profiles and 15 minutes to composite slabs with R2.
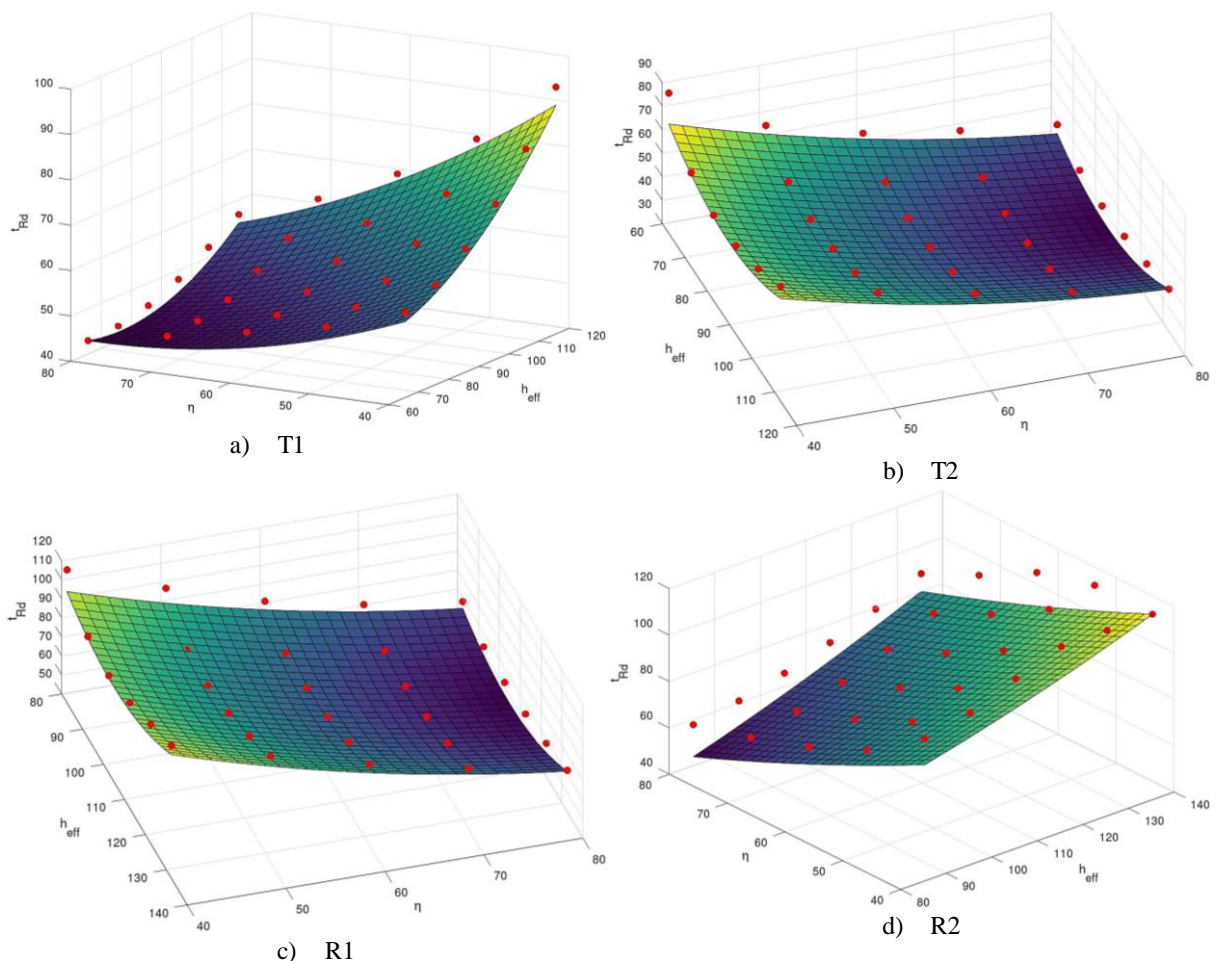
Figure 9. Comparison between the numerical results and the new proposal to determine the fire resistance of the composite slabs under investigation.

Table 6. New proposal for load bearing fire resistance.

ID	Fire resistance (t_{Rd}) calculation model	
T1	$t_{Rd} = 89.29 - 37.61x10^{-2}h_{eff} - 73.28x10^{-2}\eta + 81.94x10^{-4}h_{eff}^2 - 10.87x10^{-3}h_{eff}.\eta + 91.82x10^{-4}\eta^2$	(10)
T2	$t_{Rd} = 276.47 - 31.42x10^{-1}h_{eff} - 23.92x10^{-1}\eta + 16.65x10^{-3}h_{eff}^2 + 40.59x10^{-4}h_{eff}.\eta + 10.77x10^{-3}\eta^2$	(11)
R1	$t_{Rd} = 388.02 - 39.01x10^{-1}h_{eff} - 26.56x10^{-1}\eta + 18.75x10^{-3}h_{eff}^2 + 88.66x10^{-6}h_{eff}.\eta + 12.90x10^{-3}\eta^2$	(12)
R2	$t_{Rd} = 135.97 - 65.23x10^{-3}h_{eff} - 18.67x10^{-1}\eta + 24.33x10^{-4}h_{eff}^2 + 31.65x10^{-4}h_{eff}.\eta + 36.78x10^{-4}\eta^2$	(13)

Conclusions

This investigation presents the validation of a 3D finite element model used to determine the fire resistance of composite slabs with steel deck. Temperature and displacements are compared. The numerical results are in good agreement with experimental results, when considering the air gap effect (debonding).

In order to evaluate and characterize the influence of the load level and the effective thickness over the fire resistance of composite slabs, a parametric analysis was developed. The parameters reflect the effect of the geometry, comparing slab models with different concrete topping thickness, and also the direct effect of load level on a range from 40% to 80% of the load-bearing capacity of each composite slab model.

All the models used in the parametric study consider perfect contact between the concrete and the steel deck, consequently not considering the debonding effect as applied on the validation model, due to the uncertainty of the detachment occurrence. This model (perfect contact) also grants an extra fire safety level to the element.

Results show that the fire resistance is directly proportional to the effective thickness and inversely proportional to the loading level of the slab.

Based on the parametric study results, a new proposal has been developed to determine the fire resistance (R) of composite slabs with steel deck, according to the new quadratic proposals for both parameters. These new proposals are conservative approximations, always below the fire resistance of the numerical results.

Further works should also consider models with non-perfect contact between the concrete and the steel deck, as presented in the validation model. This should also be complemented with more experimental tests to validate the models and control with accuracy the debonding effect between materials, in terms of time and air gap thickness.

References

[1]   ECCS, Calculation of the Fire Resistance of Composite Concrete Slabs with Profiled Steel Sheet Exposed to the Standard Fire, *Fire Safety of Steel Structures*, European Convention for Constructional Steelwork - Committee T3, 1983.

[2]   G. Thomson, C. K. Moxon, R. R. Preston, *Indicative Fire Test on Composite Concrete/Steel Deck Floor System*, Steel Construction Institute, Rotherham, pp. 1987.

[3]   G. M. E. Cooke, R. M. Lawson, G. M. Newman, Fire resistance of composite deck slabs, *The Structural Engineer,* Vol. 66, No. 16, pp. 253–267, 1988.

[4]   R. Hamerlink, J. W. B. Stark, A numerical model for fire-exposed composite steel / concrete slabs, in *Proceeding of,* 115–130.

[5]   K. Both, Fire-exposed continuous span composite steel-concrete slabs, *HERON,* Vol. 41, No. 3, pp. 187-199, 1996.

[6]   CEN, EN 1994-1-2: Design of Composite Steel and Concrete Structures. Part 1-2: General Rules - Structural Fire Design, European Committee for Standardization, 2005.

[7]   L. Lim, C. Wade, *Experimental Fire Tests of Two-Way Concrete Slabs,* 722, University of Canterbury. Civil Engineering, pp. 1992.

[8]   J. Jiang, A. Pintar, J. M. Weigand, J. A. Main, F. Sadek, Improved calculation method for insulation-based fire resistance of composite slabs, *Fire Safety Journal,* Vol. 105, pp. 144-153, 2019.

[9]   P. A. G. Piloto, C. Balsa, L. Prates, R. Rigobello, The air gap effect on the fire resistance of composite slab with steel deck, in *Numerical Methods in Engineering – CMN*, 2019, pp. 610–624.

[10]   P. A. G. Piloto, C. Balsa, F. Ribeiro, R. Rigobello, Computational Simulation of the Thermal Effects on Composite Slabs Under Fire Conditions, *Mathematics in Computer Science,* Vol. 15, No. 1, pp. 155-171, 2020.

[11]   P. A. G. Piloto, C. Balsa, L. M. C. Santos, É. F. A. Kimura, Effect of the load level on the resistance of composite slabs with steel decking under fire conditions, *Journal of Fire Sciences,* Vol. 38, No. 2, pp. 212-231, 2020.

[12]   R. Hamerlinck, *The behaviour of fire-exposed composite steel/concrete slabs*, Thesis, Technische Universiteit Eindhoven, Eindhoven, 1991.

[13]   R. Hamerlinck, L. Twilt, Fire resistance of composite slabs, *Journal of Constructional Steel Research,* Vol. 33, No. 94, pp. 71–85, 1995.

[14]   P. A. G. Piloto, C. Balsa, F. Ribeiro, L. Santos, R. Rigobello, É. Kimura, Three-Dimensional Numerical Modelling of Fire Exposed Composite Slabs with Steel Deck, *MATTER: International Journal of Science and Technology,* Vol. 5, No. 2, pp. 48-67, 2019.

[15]   CEN, EN 1363-1: Fire resistance tests Part 1: General Requirements, CEN - European Committee for Standardization, 2004.

[16]   CEN, EN 1363-1: Fire resistance tests Part 1 : General Requirements, CEN-Europ, European Committee for Standardization, 2020.

[17]   CEN, EN 13501-2 Fire classification of construction products and building elements, European Committee for Standardization, 2009.

[18]   CEN, EN 1991-1-2, Eurocode 1: Actions on structures – Part 1-2: General actions – Actions on structures exposed to fire, European Committee for Standardization, 2002.

[19]   CEN, EN 1993-1-2: Design of steel structures - Part 1-2: General rules - Structural fire design Eurocode, European Committee for Standardization, 2005.

[20]   G.-Q. Li, N. Zhang, J. Jiang, Experimental investigation on thermal and mechanical behaviour of composite floors exposed to standard fire, *Fire Safety Journal,* Vol. 89, pp. 63-76, 2017.

[21]   J. Jiang, J. A. Main, J. M. Weigand, F. H. Sadek, Thermal performance of composite slabs with profiled steel decking exposed to fire effects, *Fire Safety Journal,* Vol. 95, pp. 25-41, 2018.

[22]   ISO, ISO 834-1 Fire-resistance tests - Elements of building construction, International Standard Oganization, 1999.

[23]   Y. A. Çengel, A. J. Ghajar, 2015, *Heat and Mass Transfer: Fundamentals and Applications*, McGraw-Hill, New York, 5ed.